

ON A NONLINEAR FLIGHT CONTROL LAW

Ping Lu*
Cheng Tang†

Iowa State University
Ames, IA 50011

Abstract

A methodology for nonlinear flight control law development is proposed. The control law is based on point-wise minimization of the predicted errors between the desired and actual responses of the vehicle. The control command is conveniently obtained from a fixed-point equation. Control constraints are handled without difficulty. Simulation results are provided for control of a fighter aircraft with nonlinear model.

Introduction

Traditionally, flight control systems are designed by using linear control theory. A linearized model is used to represent the dynamic behavior of the aircraft near a reference (trim) condition. The control system gains are determined based on that model. Gain scheduling, which sometimes is rather cumbersome and tends to increase the complexity of the control system, is typically employed to count for the change of the dynamics of the aircraft at different flight conditions. Although the success of the traditional approach has been tremendous, with the advance of avionics, flight-by-wire control technology and capability of onboard computers, nonlinear flight control research has increasingly received great attention. Today's high-performance aircraft often operates in regimes where nonlinearities are predominant because of high angle of attack and large angular rates. Successful nonlinear control technology has the potential of offering a relatively simple and effective solution to flight control in the entire flight envelope. A commonly cited approach in the literature for nonlinear flight control law design is dynamic inversion.

*Assistant Professor, Department of Aerospace Engineering and Engineering Mechanics.

†Graduate Student

Copyright ©1994 by the American Institute of Aeronautics and Astronautics, Inc. and the International Council of the Aeronautical Sciences. All Rights Reserved

In this approach, the nonlinearities are canceled by static feedback and the dynamics are replaced by desired linear dynamics[1]-[5]. Actual implementation of this technique in flight control system has been reported in [6]. More recently, another continuous predictive control technique has also been proposed [7]-[8]. This paper expands further on the predictive control concept. In particular, a better way of handling the control constraints is developed.

This paper is organized as follows: the next section describes a functional expansion for predicting the local response of a dynamic system; then a point-wise optimal control law subject to the constraints of bounded controls is derived. The control law is applied to a nonlinear model of a fighter aircraft. Simulation results are provided. The final section summarizes the work.

Control Law Development

Let us consider the nonlinear equations of motion of an aircraft:

$$\dot{x}_1 = f_1(x) \tag{1}$$

$$\dot{x}_2 = f_2(x) + B_2(x)u \tag{2}$$

where $x_1 \in R^{n_1}$ and $x_2 \in R^{n_2}$, $n = n_1 + n_2$ and $x = (x_1^T \ x_2^T)^T$ is the state vector which describes the translational as well as the rotational motion. $f_1 : R^n \rightarrow R^{n_1}$ are continuously differentiable nonlinear functions, representing the kinematic relationships; $f_2 : R^n \rightarrow R^{n_2}$ and $B_2 : R^n \rightarrow R^{n_2 \times m}$ are at least piecewise continuously differentiable. Equations (2) are the dynamic equations. The control vector u consists of the control surface deflections and propulsion control, and $u(t) \in U = \{u(t) \in R^m \mid L_i \leq u_i(t) \leq U_i\}$, where the bounds L_i and U_i are specified. We assume $m \leq n$. For aircraft, the second order derivative of each component of x_1 contains components of u explicitly, and the first order derivative of each component of x_2 depends on components of u explicitly.

Suppose that the desired response of the aircraft is specified by $x^*(t) \in R^n$, $0 \leq t \leq t_f$. To ensure $x^*(t)$ is achievable by the aircraft, we further assume that there exist an $r^*(t) \in U$ such that $x^*(t)$ and $r^*(t)$ satisfy the system equations (1)-(2), although no explicit knowledge of $r^*(t)$ will be needed. If at an arbitrary instant $t \in [0, t_f]$, $x(t)$ is known, then the current control $u(t)$ determines the system response in the immediate future. Specifically, consider the response $x(t+h)$, where $h > 0$ is a small time increment. We may predict $x_1(t+h)$ by a second-order Taylor series expansion at t , and $x_2(t+h)$ by a first-order expansion:

$$\begin{aligned} x_1(t+h) &\approx x_1(t) + hf_1(x(t)) \\ &+ \frac{h^2}{2}[F_{11}(x(t))f_1(x(t)) + F_{12}(x(t))f_2(x(t)) \\ &+ F_{12}(x(t))B_2(x(t))u(t)] \end{aligned} \quad (3)$$

$$x_2(t+h) \approx x_2(t) + h[f_2(x(t)) + B_2(x(t))u(t)] \quad (4)$$

where $F_{11} = \partial f_1(x(t))/\partial x_1$ and $F_{12} = \partial f_1(x(t))/\partial x_2$ (the derivative of a scalar function with respect to x is defined as a row vector). Also, partition $x^*(t)$ accordingly into $(x_1^{*T}(t) \ x_2^{*T}(t))^T$, and expand $x_1^*(t+h)$ and $x_2^*(t+h)$ in similar ways:

$$x_1^*(t+h) \approx x_1^*(t) + hx_1^*(t) + \frac{h^2}{2}\ddot{x}_1^* \quad (5)$$

$$x_2^*(t+h) \approx x_2^*(t) + hx_2^* \quad (6)$$

The error at $t+h$ can then be approximated by

$$\begin{aligned} e_1(t+h) &= x_1(t+h) - x_1^*(t+h) \\ &\approx e_1(t) + h\dot{e}_1(t) + 0.5h^2[F_{11}(x)f_1(x) \\ &+ F_{12}(x)f_2(x) + F_{12}(x)B_2(x)u \\ &- \ddot{x}_1^*] \end{aligned} \quad (7)$$

$$\begin{aligned} e_2(t+h) &= x_2(t+h) - x_2^*(t+h) \\ &\approx e_2(t) + h(f_2(x) + B_2(x)u - \dot{x}_2^*) \end{aligned} \quad (8)$$

where the dependence of $x(t)$, $x^*(t)$ and $u(t)$ on t in the right hand sides of the Eqs. (7) and (8) has been suppressed for simplicity. To determine the control $u(t)$, let us consider the minimization of the following performance index:

$$J = \frac{1}{2}e_1^T(t+h)Q_1e_1(t+h) + \frac{1}{2}e_2^T(t+h)Q_2e_2(t+h) \quad (9)$$

where Q_1, Q_2 are positive semi-definite matrices with appropriate dimensions. Taking into account the bounds on the controls and replacing $e_1(t+h)$ and $e_2(t+h)$ by Eqs. (7) and (8), we have a constrained parameter optimization problem defined by

$$\begin{aligned} \min_{u(t) \in U} J &= \min_{u(t) \in U} \frac{1}{2}\{e_1(t) + h\dot{e}_1(t) \\ &+ 0.5h^2[F_{11}(x)f_1(x) + F_{12}(x)f_2(x) \\ &+ F_{12}(x)B_2(x)u - \ddot{x}_1^*]^T Q_1\{e_1(t) \\ &+ h\dot{e}_1(t) + 0.5h^2[F_{11}(x)f_1(x) \\ &+ F_{12}(x)f_2(x) + F_{12}(x)B_2(x)u - \ddot{x}_1^*]\} \\ &+ \frac{1}{2}\{e_2(t) + h(f_2(x) + B_2(x)u \\ &- \dot{x}_2^*)^T Q_2\{e_2(t) + h(f_2(x) \\ &+ B_2(x)u - \dot{x}_2^*)\} \end{aligned} \quad (10)$$

This is a so-called quadratic programming problem. Various sophisticated algorithms exist which can be used to find the solution of problem (10). Most of them involve finding an associated m -dimensional Lagrange multiplier vector arising from the necessary conditions of optimality for such problems[10]. However, for onboard application, it is highly desirable that the implementation of the algorithm be the simplest. Motivated by the work in Ref. [9], we give a simple and efficient algorithm for solving problem (10). Let us first define a vector function $s: R^m \rightarrow U$ with its i th component defined as a saturation function of the i th component of its argument

$$s_i(q) = \begin{cases} U_i, & q_i \geq U_i \\ q_i, & L_i < q_i < U_i \\ L_i, & q_i \leq L_i \end{cases} \quad (11)$$

for any $q \in R^m$. Next, denote

$$\begin{aligned} P &= 0.25h^2(F_{12}B_2)^T Q_1 F_{12}B_2 + h^2 B_2^T Q_2 B_2 \quad (12) \\ z &= 0.5h^2(F_{12}B_2)^T Q_1 \{0.5h^2[\ddot{x}_1^* - F_{11}(x)f_1(x) \\ &- F_{12}(x)f_2(x) - e_1(t) + h\dot{e}_1(t)]\} \\ &+ hB_2^T Q_2 \{h[\dot{x}_2^* - f_2(x)] - e_2(t)\} \end{aligned} \quad (13)$$

Then we have the following result.

Theorem:

For the given $Q_1 \geq 0, Q_2 \geq 0$, suppose that the $m \times m$ matrix P defined in Eq. (12) is positive definite at $x(t)$. The unique optimal control $u^*(t)$ to problem (10) for any $h > 0$ satisfies the fixed-point equation

$$u = s[\beta z - (\beta P - I)u] \quad (14)$$

where I is an $m \times m$ identity matrix, and $\beta > 0$ is calculated from the elements of the P matrix

$$\beta = \left\{ \sum_{i=1}^m \sum_{j=1}^m p_{ij}^2 \right\}^{-1/2} \quad (15)$$

Moreover, the mapping

$$\rho(u) = s[\beta z - (\beta P - I)u] \quad (16)$$

is a global contraction mapping in R^m . Therefore the fixed-point iteration sequence $\{u^k\}$ generated from

$$u^{k+1} = \rho(u^k), \quad k = 0, 1, 2, \dots, \forall u^0 \in R^m \quad (17)$$

converges to the optimal control $u^*(t)$.

The proof of the Theorem is based on the necessary and sufficient conditions for problem (10) [10] and the unique structure of the control constraint set U . The detailed proof will be reported in another forthcoming paper.

Remarks:

1. Since the instant t is arbitrary, Eq. (14) provides a continuous nonlinear feedback control that is optimal in the sense of Eq. (10). This is particularly meaningful when some of the control components are saturated. In contrast, simple saturations were used in Ref. [7], which in general is not optimal; the dynamic inversion approach will not be valid at all when control saturation is encountered.
2. When $u^*(t)$ is in the interior of U , a closed-form solution can be obtained [7]. But since the fixed-point iteration (17) converges rapidly in both saturated and unsaturated cases, $u^*(t)$ can simply be obtained from (17) in any case.
3. The parameter h serves as a controller parameter, and it need not be as small as the "integration step size". For more discussion on the roll of h as a measure of the controller gain and time-constant of the closed-loop system, we refer the reader to Ref. [7].

Flight Control of a Fighter Aircraft

Aircraft Model

The model of the aircraft is taken from Ref. [11]. The equations of motions are given as

$$\dot{\alpha} = q + \frac{g}{V} \cos \gamma - \frac{\bar{q}S}{mV} C_L - \frac{T_x}{mV} \sin \alpha \quad (18)$$

$$\dot{V} = -g \sin \gamma - \frac{\bar{q}S}{m} C_D + \frac{T_x}{m} \cos \alpha \quad (19)$$

$$\dot{q} = \frac{1}{I_y} [I_{z_0} T_x + \bar{q}S(\bar{c}C_m + d_L C_L + d_D C_D)] \quad (20)$$

$$\dot{\theta} = q \quad (21)$$

$$\dot{y} = V \sin \gamma \quad (22)$$

where

$$d_L(\alpha) = I_x \cos \alpha + I_z \sin \alpha \quad (23)$$

$$d_D(\alpha) = I_x \sin \alpha + I_z \cos \alpha \quad (24)$$

$$\gamma = \theta - \alpha \quad (25)$$

The state variables are angle of attack α , airspeed V , pitch rate q , pitch angle θ , and altitude y . Control variables are $u_1 = \delta_h$, the stabilator deflection, and $u_2 = \tau_h$, the throttle. δ_h is restricted by the limits $-24^\circ \leq \delta_h \leq 10.5^\circ$, and τ_h by $0 \leq \tau_h \leq 1.0$. The maximum thrust in the x-direction is modelled as a function of Mach number M :

$$T_{max}(M) = 106,752 + 24,464 \sin[2.12(M - 0.7)] \quad (26)$$

$$T_x(M, \tau_h) = T_{max}(M) \cdot \tau_h(N) \quad (27)$$

The aerodynamic coefficients C_L, C_D and C_m are provided in subsonic regimes as analytical nonlinear functions of the state variables and linear functions of the control variables [11]. Therefore the state equations take the form of system (1)-(2). According to our notation, $x_1 = (\theta, y)^T$, $x_2 = (\alpha, V, q)^T$. The other physical constants are

$$I_y = 205,127 \text{ kg} - \text{m}^2 \quad I_{z_0} = 0.0711 \text{ m}$$

$$m = 15,097 \text{ kg} \quad I_x = -0.09 \text{ m}$$

$$W = mg = 147,950.6 \text{ N} \quad I_z = 0.0711 \text{ m}$$

$$S = 37.16 \text{ m}^2, \quad \bar{c} = 3.51 \text{ m}$$

Maneuver I: Changing Trim Conditions

Suppose that the aircraft is initially flying along the constant-speed level trajectory at $y_0 = 4,800 \text{ m}$ with $M = 0.4$. The trim conditions are

$$y_0 = 4,800 \text{ m}, M_0 = 0.4, \theta_0 = \alpha_0 = 5.186^\circ, q_0 = 0 \quad (28)$$

Now the flight conditions are to be changed to another set of trim conditions

$$y^* = 5,000 \text{ m}, M^* = 0.7, \theta^* = \alpha^* = 1.29^\circ, q^* = 0 \quad (29)$$

The control law (14) is used for computation of u_1 and u_2 . The parameter h is set at a constant value of 1.0 (sec). The weighting matrices Q_1 and Q_2 are diagonal matrices with all elements on the main diagonal being positive. Fixed-point iteration (17) is implemented to solve for the controls. With the previously obtained value as the initial iteration point, convergence with an accuracy of 10^{-3} was achieved just in one iteration every time when the controls were calculated. Figures 1-3 show the variations of $y(t)$, $\theta(t)$, $\alpha(t)$, and $V(t)$. Figures 4-5 give the histories of the two controls. Notice the initial saturation of the throttle.

Maneuver II: Pitch Orientation Control

The proposed control law is flexible in that different control objectives may be accomplished by setting the controller parameters accordingly. For instance, in the pitch orientation control, the aircraft is commanded to achieve certain pitch rate while the airspeed is maintained constant. A traditional approach is to design the inner loop of the autopilot for the pitch-rate control, and the outer loop for the Mach-hold[12]. In the current approach, one only needs to set $Q_1 = 0$, the two weightings corresponding to q and V in Q_2 to be positive, and others zero in Q_2 . Then from the derivation, one can easily see that only V and q will be controlled to track their desired values. Suppose that the aircraft is initially in trim conditions

$$y_0 = 5,000 \text{ m}, M_0 = 0.4, \theta_0 = \alpha_0 = 5.424^\circ, q_0 = 0 \quad (30)$$

The pitch-rate command is

$$q^* = \begin{cases} 5 \text{ (deg/sec)}, & 0 \leq t \leq 5 \text{ (sec)} \\ -5 \text{ (deg/sec)}, & 5 < t \leq 10 \text{ (sec)} \end{cases} \quad (31)$$

and $V^* = 131.9 \text{ m/sec}$ ($M = 0.4$). The response of the pitch rate $q(t)$ is depicted in Fig. 6, the variation of $V(t)$ is shown in Fig. 7, and the corresponding variations of $\theta(t)$ and $\alpha(t)$ are in Fig. 8. It is seen that the velocity varies less than one m/sec while q is changing to the desired level, despite the throttle saturation observed in Fig. 9. The stabilator deflection history is given in Fig. 10.

Maneuver III: Pitch Angle Control

In this maneuver a desired pitch attitude is to be achieved while maintaining the speed. Again, suppose that the initial conditions are the same as in Eq. (30). Let

$$\theta^* = 30^\circ, V^* = 131.9 \text{ m/sec} \quad (32)$$

As in Maneuver II, set positive weightings corresponding to θ and V , zero weightings for the others. Figure 11 shows the responses of $\theta(t)$ and $\alpha(t)$. The speed response $V(t)$ is plotted in Fig. 12. Again, very little variation in the speed occurred while the pitch attitude reached the desired value. The altitude history is in Fig. 13. The corresponding stabilator deflection and throttle histories are shown in Figs. 14-15, respectively.

Conclusion

A methodology for nonlinear flight control law design is presented. The control is based on point-wise

minimization of the predicted errors between the desired and actual responses of the vehicle. The control command is conveniently solved from a fixed-point equation. Control constraints are handled without difficulty. In the case of control saturation, the control law still has a clear physical meaning: it is still the optimal control within the control set, optimal in the sense of the point-wise minimization. Simulation of several maneuvers for a nonlinear fighter aircraft is provided. The control law demonstrates satisfactory performance in the tests.

References

- [1] Snell, S. A., Enns, D. F., and Garrard, W. L., "Nonlinear Inversion Flight Control for a Supermaneuverable Aircraft", *Journal of Guidance, Control, and Dynamics*, Vol. 15, No. 4, pp. 976-984, 1992.
- [2] Lane, S. H., and Stengel, R. F., "Flight Control Design Using Nonlinear Inverse Dynamics", *Automatica*, Vol. 24, No. 4, July, 1988, pp. 471-483.
- [3] Meyer, G., Su, R., and Hunt, L. R., "Application of Nonlinear Transformation to Automatic Flight Control", *Automatica*, Vol. 20, No. 1, pp. 103-107, 1984.
- [4] Menon, P. K. A., Badgett, M. E., Walker, R. A., and Duke, E. L., "Nonlinear Flight Test Trajectory Controls for Aircraft", *Journal of Guidance, Control, and Dynamics*, Vol. 10, No. 1, pp. 62-77, 1987.
- [5] Wise, K. A., "Nonlinear Aircraft Flight Control Using Dynamic Inversion", *Proceedings of American Control Conference*, Chicago, Illinois, June 1992.
- [6] Franklin, J. A., Hynes, C. S., Hardy, G. H., Martin, J. L., and Innis, R. C., "Flight Evaluation of Augmented Controls for Approach and Landing of Powered-Lift Aircraft", *Journal of Guidance, Control, and Dynamics*, Vol. 9, No. 5, pp. 555-565, 1986.
- [7] Lu, P., "Nonlinear Predictive Controllers for Continuous Systems", to appear in *Journal of Guidance, Control, and Dynamics*, Vol. 17, No. 3, 1994.
- [8] Khan, M.A., and Lu, P., "A New Technique for Nonlinear Control of Aircraft," to appear in *Journal of Guidance, Control, and Dynamics*, 1994.

- [9] R. D. Barnard, "Continuous-Time Implementation of Optimal-Aim Controls", *IEEE Trans. Automat. Contr.*, vol. AC-21, pp. 432-434, 1976.
- [10] R. Fletcher, *Practical Methods of Optimization*, 2nd Edition, John Wiley and Sons, New York, 1989.
- [11] H. Stalford, and E. Hoffman, "Maximum Principle Solutions for Time-Optimal Half-Loop Maneuvers of a High Alpha Fighter Aircraft", *Proceedings of the American Control Conference*, Pittsburgh, Penn., June 21-23, 1989.
- [12] J. H. Blakelock, *Automatic Control of Aircraft and Missiles*, second edition, John Wiley & Sons, New York, 1991.

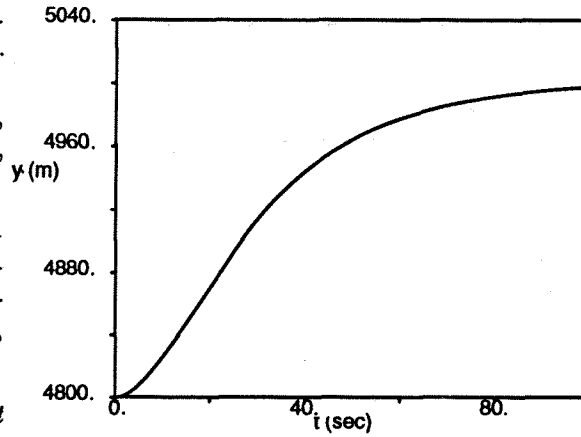


Figure 1: Maneuver I: altitude history

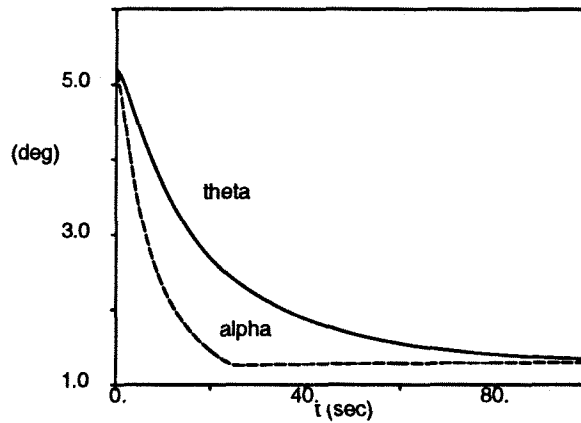


Figure 2: Maneuver I: θ and α histories

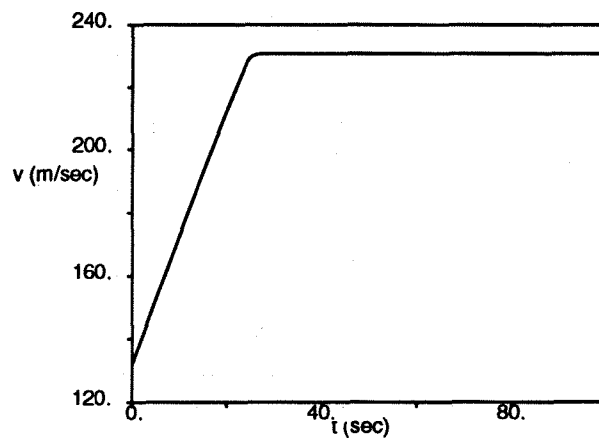


Figure 3: Maneuver I: speed history

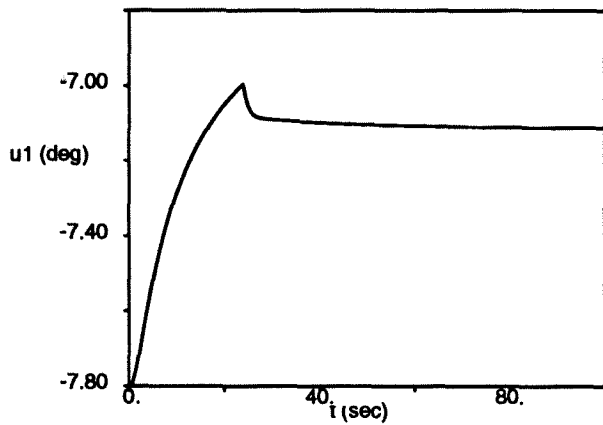


Figure 4: Maneuver I: stabilator deflection history

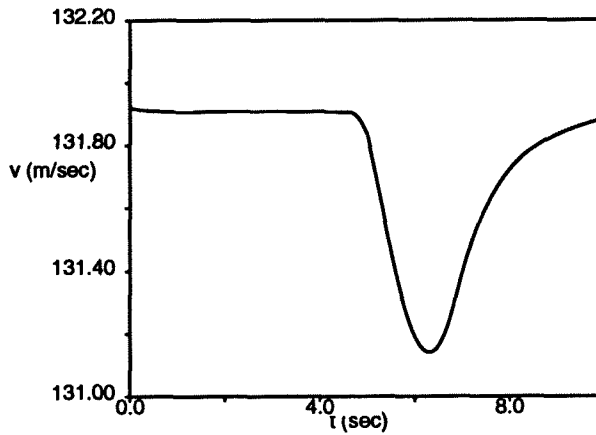


Figure 7: Maneuver II: speed history

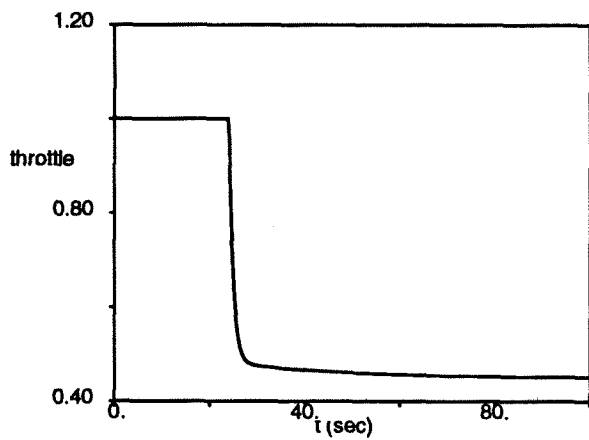


Figure 5: Maneuver I: throttle history

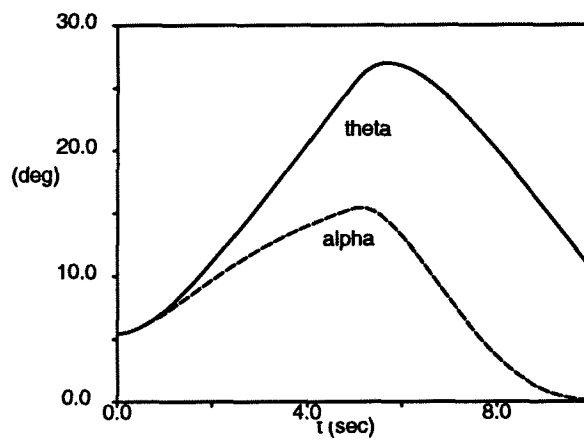


Figure 8: Maneuver II: θ and α histories

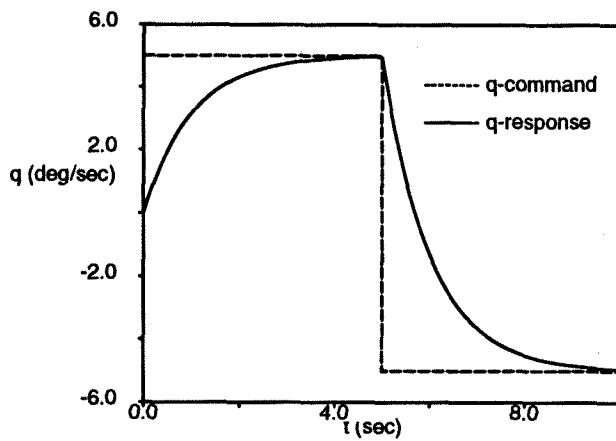


Figure 6: Maneuver II: pitch rate history

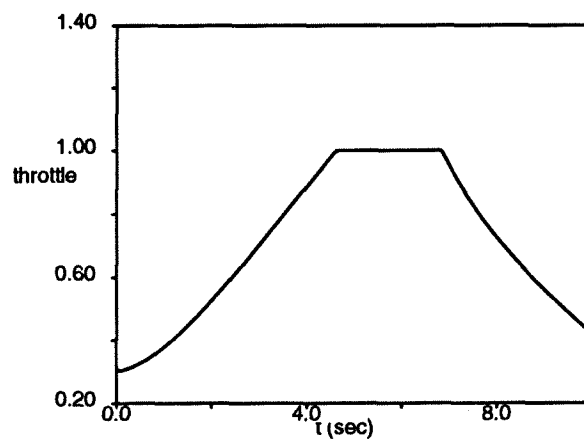


Figure 9: Maneuver II: throttle history

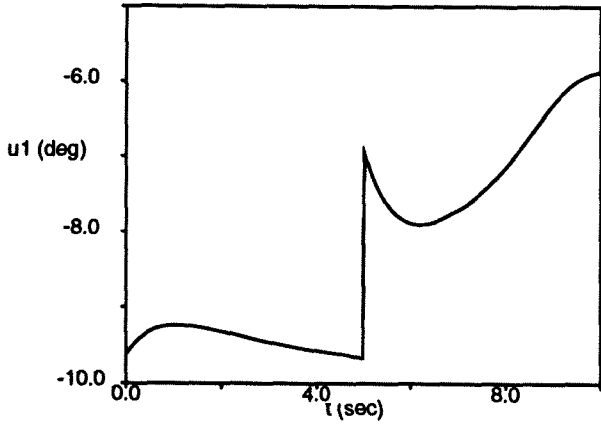


Figure 10: Maneuver II: stabilator deflection

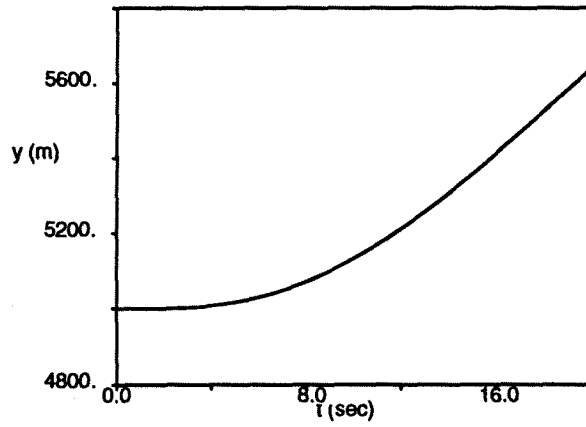


Figure 13: Maneuver III: altitude history

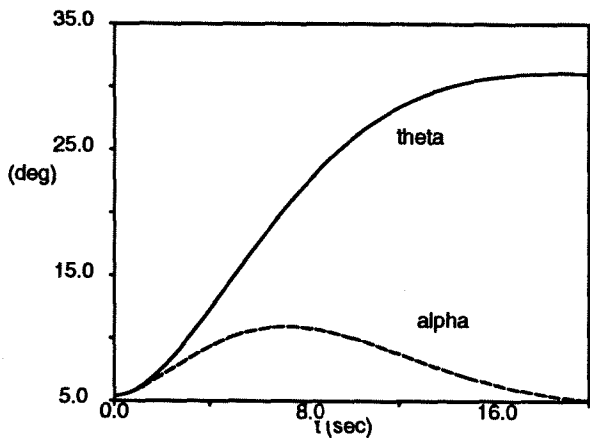


Figure 11: Maneuver III: θ and α histories

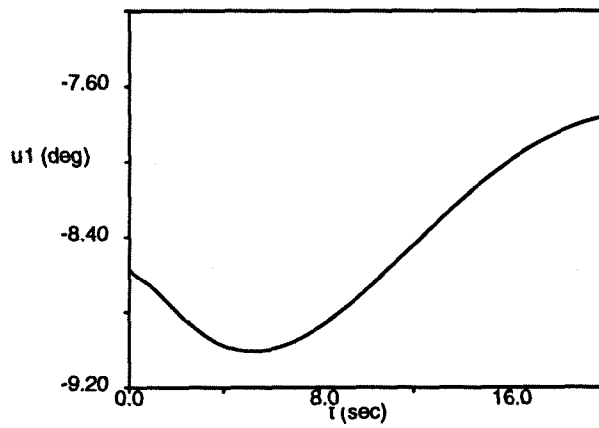


Figure 14: Maneuver III: stabilator deflection

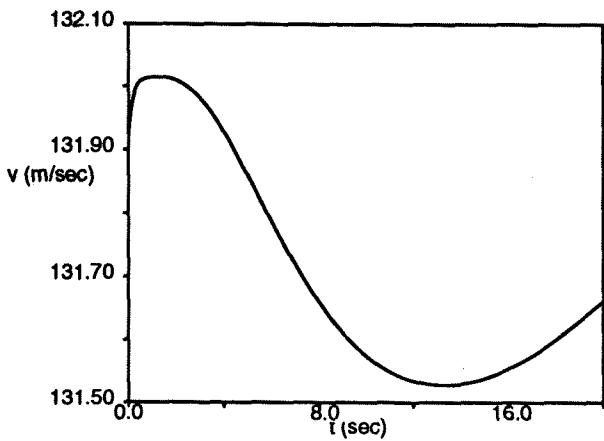


Figure 12: Maneuver III: speed history

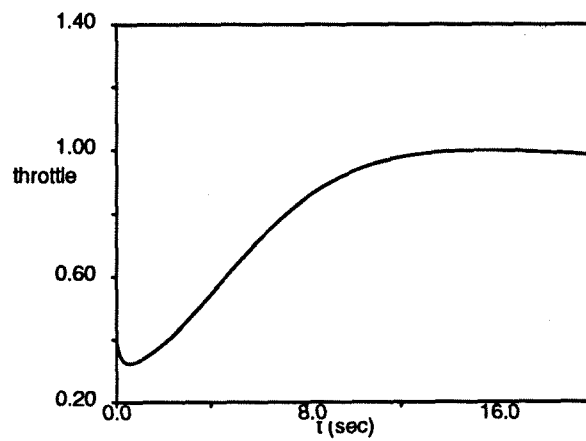


Figure 15: Maneuver III: throttle history